Mechanisms for the $T=\frac{1}{2}$ and $T=\frac{3}{2}$ Recurrences

P. R. AUVIL AND J. J. BREHM
Northwestern University, Evanston, Illinois
(Received 19 May 1965)

The conjecture that inelastic states containing an f meson should provide a natural-recurrence mechanism is investigated. We first treat coupled $N\pi$ and N_Rf channels where, in seeking a recurrence, N_R denotes the previous recurrence. We establish that the attraction is always maximal for angular momentum and parity corresponding to the recurrence state. We concentrate on the $\frac{7}{2}^+(T=\frac{3}{2})$ and $\frac{9}{2}^+(T=\frac{1}{2})$ states, and find that the attraction is strong enough to produce resonances, in fact, as we have computed it, excessively so. We then consider coupled $N_R\pi$ and N_Rf states, and look for these resonances to occur in $N_R\pi$ scattering. The resonance positions determined by taking this point of view are vastly improved. In particular, if we invoke a static version of $SU(6)$ symmetry we obtain a $\frac{7}{2}^+(T=\frac{3}{2})$ resonant state in good agreement with observation.

I. INTRODUCTION

THE spectra of states in πN scattering for isospins $T=\frac{1}{2}$ and $\frac{3}{2}$ exhibit many resonances.[1] Of those having determined or suggested quantum numbers, we may classify all but two according to the notion of recurrences.[2] The two families of recurrences (for $T=\frac{1}{2}$ and $\frac{3}{2}$) are shown in Table I; the two observed resonances, omitted in the classification, are the $\frac{3}{2}^-$ ($T=\frac{1}{2}$, 1512 MeV) and the ? ($T=\frac{1}{2}$, 2700 MeV). In the $T=\frac{1}{2}$ channel we shall consider the states $\frac{5}{2}^+$ (1688 MeV) and $\frac{9}{2}^+$ (2190 MeV); if the latter of these turns out experimentally to have the indicated J^P assignment then these two states would indeed be the first and second recurrences of the nucleon. In the $T=\frac{3}{2}$ channel the (3,3) isobar recurs in the $\frac{7}{2}^+$ resonant state at 1920 MeV; the resonance at 2360 MeV would then be the next recurrence if its quantum numbers were established to be $J^P=11/2^+$.

We have recently proposed a dynamical model which yields the $\frac{5}{2}^+$ ($T=\frac{1}{2}$) resonance[3]; at the same time we conjectured how that model might be extended to obtain all of the recurrences for either isospin. In this paper we shall implement that conjecture with the necessary calculations, and, in addition, we shall present a device for extending the model of Ref. 3 which yields an improved set of results for the other recurrences.

TABLE I. The $T=\frac{1}{2}$ and $T=\frac{3}{2}$ recurrences.

$T=\frac{1}{2}$		$T=\frac{3}{2}$	
J^P	Mass (MeV)	J^P	Mass (MeV)
$\frac{1}{2}^+$	939	$\frac{3}{2}^+$	1238
$\frac{5}{2}^+$	1688	$\frac{7}{2}^+$	1920
$\frac{9}{2}^+$?	2190	$11/2^+$?	2360

[1] The knowledge of these that is available at the present time may be found in A. H. Rosenfeld, A. Barbaro-Galtieri, W. H. Barkas, P. L. Bastien, J. Kirz, and M. Roos, Rev. Mod. Phys. **36**, 977 (1964). References to the various experiments are given there.

[2] We hasten to point out that we are in no way invoking Reggeism for the purposes of calculation; we are only borrowing a concept, that of recurrence, which is an outgrowth of Reggeism. See, e.g., G. F. Chew and S. C. Frautschi, Phys. Rev. Letters **8**, 41 (1962); R. Blankenbecler and M. L. Goldberger, Phys. Rev. **126**, 766 (1962).

Our models are based on two-channel unitarity; in Fig. 1 we indicate the choice of inelastic state which, according to the original conjecture,[3] we couple to the $N\pi$ channel. In the figure the inelastic state contains the particles N_R and f where f denotes the 2^+ ($T=0$) meson of mass 1250 MeV and where N_R denotes the previous recurrence in the isospin channel of interest. That is, for the $\frac{5}{2}^+$ ($T=\frac{1}{2}$) state we have taken N_R to be the nucleon[3]; for the $\frac{9}{2}^+$ ($T=\frac{1}{2}$) state (we are assuming J^P such that we have another recurrence) we take N_R to be $\frac{5}{2}^+$; for the $\frac{7}{2}^+$ ($T=\frac{3}{2}$) state we take N_R to be the (3,3) isobar. In every case the f meson serves to add the two units of angular momentum necessary for recurrences.

It is well known[4,5] that absorption through inelastic s states provides a most efficient mechanism for attractive elastic scattering; the appeal of using these states which are virtual at the resonance energy has been pointed out by Cook and Lee.[4] Every amplitude of interest to us here has positive parity; hence we may assume s-wave absorption. Given that the inelastic states have $L=0$, the recurrence state then corresponds to the maximum allowable total angular momentum. We shall show that this is the most attractive configuration. We follow the example of Ref. 4 and choose the forces to be purely absorptive; as indicated in Fig. 1, we take the one-pion-exchange diagram to provide the dominant coupling be-

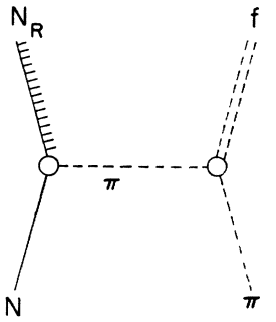

FIG. 1. π-exchange coupling $N\pi$ to N_Rf.

[3] P. R. Auvil and J. J. Brehm, Phys. Rev. **138**, B458 (1965).
[4] L. F. Cook and B. W. Lee, Phys. Rev. **127**, 283 (1962); **127**, 297 (1962).
[5] F. T. Meiere, Phys. Rev. **136**, B1196 (1964).

tween channels. The application of this model, the conjecture of Ref. 3, is the subject of Sec. II. In this section we give the calculation of the necessary spin-dependent vertex factors and the projection of the diagram into the relevant J^P amplitudes. The results of the model are computed for the $\frac{7}{2}^+$ ($T=\frac{3}{2}$) and the $\frac{9}{2}^+$ ($T=\frac{1}{2}$) states.

The pursuit of this program yields the conclusion that the attraction is sufficient to support our conjecture. In fact, by our method of computing the strength of the forces, the attraction is excessive in that these two resonant states appear at energies well below their experimental values. At this juncture a different point of view is adopted for the dynamics of these two states, In Sec. III we treat coupled $N_R\pi$ and N_Rf channels, and we explain why these may provide a dynamical model which is a more relevant extension of the mechanism of Ref. 3. In Fig. 2 we indicate the assumed coupling of the two channels. In Sec. IV we conclude with some remarks suggesting how the results of Sec. III are reflected in $N\pi$ scattering.

II. THE COUPLED $N\pi$, N_Rf PROBLEM

A. The Model and Its Solution

We denote the coupled $N\pi$ and N_Rf channels by the subscripts 1 and 3, respectively, (we reserve the subscript 2 for the $N_R\pi$ channel). The amplitudes for angular momentum and parity J^P are described by the matrix

$$\mathfrak{M}=\begin{pmatrix} M_{11} & M_{13}{}^{\xi} \\ M_{31}{}^{\eta} & M_{33}{}^{\eta\xi} \end{pmatrix} \tag{1}$$

in which we have suppressed the J^P index. We have also suppressed the index j denoting the spin of N_R. The superscripts η and ξ run through $\frac{5}{2}(2j+1)$ integers corresponding to the number of different J^P eigenamplitudes. In Table II we identify the off-diagonal block M_{31} of $\mathfrak{M}$ in terms of the helicity amplitudes,[4,6] for positive parity. The helicity amplitudes in turn are given by

$$\langle\alpha,\lambda|M_{31}|\beta\rangle=2\pi\int_{-1}^{1}d\cos\theta d_{\alpha-\lambda,\beta}{}^{J}(\theta)M_{31}, \tag{2}$$

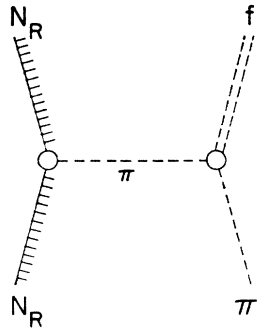

FIG. 2. π-exchange coupling $N_R\pi$ to N_Rf.

where the helicities and the choice of c.m. coordinate system are as shown in Fig. 3.

To incorporate the correct threshold behavior we define

$$\mathfrak{F}=\begin{pmatrix} F_{11} & F_{13}{}^{\xi} \\ F_{31}{}^{\eta} & F_{33}{}^{\eta\xi} \end{pmatrix}, \tag{3}$$

where, for example,

$$F_{11}=\frac{2m}{p_0+m}\left(\frac{p_0+m}{p}\right)^{2l}M_{11}, \tag{4}$$

$$F_{31}{}^{\eta}=\left(\frac{2m}{p_0+m}\right)^{1/2}\left(\frac{2M}{Q_0+M}\right)^{1/2}\left(\frac{p_0+m}{p}\right)^{l}M_{31}{}^{\eta}, \tag{5}$$

in which (m,p,p_0) and (M,Q,Q_0) denote the (mass, momentum, energy) of N and N_R, respectively. We denote the π and f masses by μ and Δ. In Eqs. (4) and (5) we take $l=3$ for the $\frac{7}{2}^+$ state and $l=5$ for the $\frac{9}{2}^+$ state; note that we have used $L=0$ in the inelastic state.

TABLE II. J^P eigenamplitudes in terms of helicity amplitudes.

η	Combinations for positive parity J^+
1	$\langle j,2\|M_{31}\|\frac{1}{2}\rangle+(-)^{J-j}\langle -j,-2\|M_{31}\|\frac{1}{2}\rangle$
2	$\langle j-1,2\|M_{31}\|\frac{1}{2}\rangle+(-)^{J-j}\langle -(j-1),-2\|M_{31}\|\frac{1}{2}\rangle$
...	...
$2j+1$	$\langle -j,2\|M_{31}\|\frac{1}{2}\rangle+(-)^{J-j}\langle j,-2\|M_{31}\|\frac{1}{2}\rangle$
$2j+2$	$\langle j,1\|M_{31}\|\frac{1}{2}\rangle+(-)^{J-j}\langle -j,-1\|M_{31}\|\frac{1}{2}\rangle$
...	...
$2(2j+1)$	$\langle -j,1\|M_{31}\|\frac{1}{2}\rangle+(-)^{J-j}\langle j,-1\|M_{31}\|\frac{1}{2}\rangle$
$4j+3$	$\langle j,0\|M_{31}\|\frac{1}{2}\rangle+(-)^{J-j}\langle -j,0\|M_{31}\|\frac{1}{2}\rangle$
...	...
$\frac{5}{2}(2j+1)$	$\langle\frac{1}{2},0\|M_{31}\|\frac{1}{2}\rangle+(-)^{J-j}\langle -\frac{1}{2},0\|M_{31}\|\frac{1}{2}\rangle$

The model employs the many-channel N/D method[7] in which we let

$$\mathfrak{F}=\mathfrak{N}\mathfrak{D}^{-1}, \tag{6}$$

where the elements of the matrices $\mathfrak{N}$ and $\mathfrak{D}$ are expressed in the notation of Eqs. (1) and (3), and where

$$\text{disc}\mathfrak{D}=-2\pi i\rho\mathfrak{N} \tag{7}$$

on the right-hand cuts. The matrix of phase-space factors is diagonal:

$$\rho=\begin{pmatrix} \rho_1 & 0 \\ 0 & \rho_3\delta_{\eta\xi} \end{pmatrix} \tag{8}$$

and, apart from θ functions, we have

$$\rho_1=\frac{2}{(4\pi)^3}\frac{p^{2l+1}}{w(p_0+m)^{2l-1}}, \qquad \rho_3=\frac{2}{(4\pi)^3}Q(Q_0+M)/w. \tag{9}$$

[6] M. Jacob and G. C. Wick, Ann. Phys. (N. Y.) **7**, 404 (1959).

[7] R. Blankenbecler, Phys. Rev. **122**, 983 (1961).

In terms of these quantities the S matrix is

$$S=1+2\pi i\rho^{1/2}\mathfrak{F}\rho^{1/2}. \tag{10}$$

We define the model by specifying the discontinuity of $\mathfrak{F}$ on the left-hand cuts in a pole approximation as

$$\begin{aligned}&\mathrm{disc}_L F_{11}=0=\mathrm{disc}_L F_{33}{}^{\eta\xi},\\ &\mathrm{disc}_L F_{31}{}^{\eta}=2\pi i d_\eta\delta(w-w_1),\\ &\mathrm{disc}_L F_{13}{}^{\xi}=2\pi i d_\xi\delta(w-w_1).\end{aligned} \tag{11}$$

The presence of the δ functions in (11) reduces the solution of the model to an algebraic problem. Since we are looking for resonances below the inelastic threshold the only quantity we need is the determinant of the $\mathfrak{D}$ matrix:

$$\mathfrak{D}_0\equiv\det\mathfrak{D}=1-d^2(w-w_1)^2R_1(w)T_1(w) \tag{12}$$

in which

$$d^2=\sum_\eta d_\eta{}^2 \tag{13}$$

and where

$$\begin{aligned}R_1(w)&=\int_{m+\mu}^{\infty}\frac{dx}{(x-w)}\frac{\rho_1(x)}{(x-w_1)^2}\\ \text{and}\qquad\\ T_1(w)&=\int_{M+\Delta}^{\infty}\frac{dx}{(x-w)}\frac{\rho_3(x)}{(x-w_1)^2}.\end{aligned} \tag{14}$$

The criterion for a resonance at an energy w^* below the inelastic threshold is

$$\mathrm{Re}\mathfrak{D}_0(w^*)=0. \tag{15}$$

The model contains two parameters w_1 and d^2. We determine these by explicit evaluation of the diagram of Fig. 1. Such a calculation yields a singularity in F_{31} at $w=m+\mu$. This circumstance is attributable to two sources: first, the threshold factor in (5), and second, the analytic continuations necessary to define F_{31} with unstable N_R and f particles.[4] This singularity is in general not a simple pole so if we take $w_1=m+\mu$ we cannot determine d^2 by computing the residue at the pole. If the model is to make any sense we must find our resonance between the two thresholds; thus we choose the inelastic threshold as a representative (and also very convenient) point for the evaluation of the coefficient:

$$d_\eta=(w_1-w_3)[F_{31}{}^{\eta}(w_3)]_{\text{diagram}} \tag{16}$$

with $w_3=M+\Delta$.

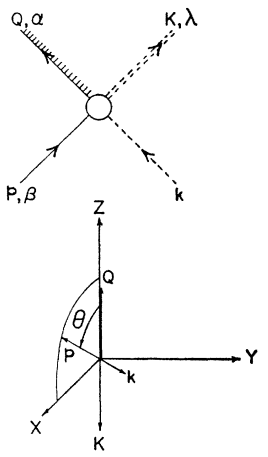

FIG. 3. Definition of the kinematic variables.

TABLE III. Angular-momentum amplitudes for $L=0$ and for each N_R.

$N_R=\frac{3}{2}^+$		$N_R=\frac{5}{2}^+$	
J^+	l	J^+	l
$\frac{1}{2}^+$	1	$\frac{1}{2}^+$	1
$\frac{3}{2}^+$	1	$\frac{3}{2}^+$	1
$\frac{5}{2}^+$	3	$\frac{5}{2}^+$	3
$\frac{7}{2}^+$	3	$\frac{7}{2}^+$	3
		$\frac{9}{2}^+$	5

B. The Coupling Parameters of the Model

We now consider the two problems of interest separately; in the first instance we take $N_R=\frac{3}{2}^+$ with $T=\frac{3}{2}$, and in the second $N_R=\frac{5}{2}^+$ with $T=\frac{1}{2}$. If we suppress all but $L=0$ in the N_Rf state and consider only positive parity, then the amplitudes listed for each choice of N_R in Table III are relevant.

We depart from the approach of Cook and Lee, and regard N_R and f each as single particles; for this purpose we need the appropriate N_R and f wave functions. These are given in Tables IV, V, and VI. The e's and u's are the usual spin-1 and spin-$\frac{1}{2}$ wave functions in the helicity basis:

$$\begin{aligned}&e^{\pm1}(Q)=\mp(1,\pm i,0;0)/\sqrt{2},\\ &e^{0}(Q)=(0,0,Q_0;iQ)/M,\end{aligned} \tag{17}$$

$$u_{\pm1/2}(Q)=\left(\frac{Q_0+M}{2M}\right)^{1/2}\begin{pmatrix}\chi_\pm\\ \pm[Q/(Q_0+M)]\chi_\pm\end{pmatrix} \tag{18}$$

in which $\chi^\dagger\chi=1$. The expressions (17) and (18) are referred to the orientation of the coordinate system as given in Fig. 3; states corresponding to other directions of the momenta can be obtained by applying rotation operators.

According to Eq. (16) we need only compute the diagram of Fig. 1 at the inelastic threshold. Here both

TABLE IV. The 5-component wave function $\phi^\lambda(K)$ for the 2^+ particle.

$$\begin{aligned}\phi^2&=e^1(K)e^1(K)\\ \phi^1&=[e^1(K)e^0(K)+e^0(K)e^1(K)]/\sqrt{2}\\ \phi^0&=[e^1(K)e^{-1}(K)+2e^0(K)e^0(K)+e^{-1}(K)e^1(K)]/\sqrt{6}\\ \phi^{-1}&=[e^0(K)e^{-1}(K)+e^{-1}(K)e^0(K)]/\sqrt{2}\\ \phi^{-2}&=e^{-1}(K)e^{-1}(K)\end{aligned}$$

TABLE V. The 4-component wave function $\psi^\alpha(Q)$ for the $\frac{3}{2}^+$ particle.

$$\psi^{3/2}=e^1(Q)u_{1/2}(Q)$$
$$\psi^{1/2}=[e^1(Q)u_{-1/2}(Q)+\sqrt{2}e^0(Q)u_{1/2}(Q)]/\sqrt{3}$$
$$\psi^{-1/2}=[\sqrt{2}e^0(Q)u_{-1/2}(Q)+e^{-1}(Q)u_{1/2}(Q)]/\sqrt{3}$$
$$\psi^{-3/2}=e^{-1}(Q)u_{-1/2}(Q)$$

TABLE VI. The 6-component wave function $\psi^\alpha(Q)$ for the $\frac{5}{2}^+$ particle.

$$\psi^{5/2}=\phi^2(Q)u_{1/2}(Q)$$
$$\psi^{3/2}=[2\phi^1(Q)u_{1/2}(Q)+\phi^2(Q)u_{-1/2}(Q)]/\sqrt{5}$$
$$\psi^{1/2}=[\sqrt{3}\phi^0(Q)u_{1/2}(Q)+\sqrt{2}\phi^1(Q)u_{-1/2}(Q)]/\sqrt{5}$$
$$\psi^{-1/2}=[\sqrt{2}\phi^{-1}(Q)u_{1/2}(Q)+\sqrt{3}\phi^0(Q)u_{-1/2}(Q)]/\sqrt{5}$$
$$\psi^{-3/2}=[\phi^{-2}(Q)u_{1/2}(Q)+2\phi^{-1}(Q)u_{-1/2}(Q)]/\sqrt{5}$$
$$\psi^{-5/2}=\phi^{-2}(Q)u_{-1/2}(Q)$$

N_R and f are at rest in the over-all c.m. system. In the following calculations it will be understood that $w=w_3$.

The $f\pi\pi$ vertex is given by

$$U_\lambda=f\phi^\lambda{}_{\mu\nu}(K)k_\mu k_\nu\,, \tag{19}$$

where f is the coupling constant. In the rest frame of f this becomes

$$U_\lambda=(-)^\lambda(\tfrac{2}{3})^{1/2}fk^2d^2{}_{\lambda,0}(\theta) \tag{20}$$

(it is convenient for later use to express the vertices in terms of Wigner d functions[8]). The width of the f resonance can be computed from (20); it is

$$\Gamma_f=\frac{1}{15}\frac{k^5}{\Delta^2}\frac{f^2}{4\pi}. \tag{21}$$

For a width of 100 MeV we obtain $f^2/4\pi=0.536\mu^{-2}$.

For the $N^*{}_{3/2}N\pi$ vertex we have

$$V_{\alpha\beta}=g_3\bar{\psi}^\alpha{}_\mu(Q)p_\mu u_\beta(p) \tag{22}$$

so that in the $N^*{}_{3/2}$ rest frame,

$$V_{\alpha\beta}=(\tfrac{2}{3})^{1/2}[(p_0+m)/2m]^{1/2}g_3pd_{\alpha,\beta}{}^{3/2}(\theta)\,. \tag{23}$$

The width is given by

$$\Gamma_{3/2}=\tfrac{1}{3}[(p_0+m)/M]p^3g_3{}^2/4\pi\,, \tag{24}$$

hence, for $\Gamma_{3/2}=125$ MeV, we have $g_3{}^2/4\pi=0.383\mu^{-2}$.

The $N^*{}_{5/2}N\pi$ vertex is

$$V_{\alpha\beta}=g_5\bar{\psi}^\alpha{}_{\mu\nu}(Q)p_\mu p_\nu\gamma_5 u_\beta(p) \tag{25}$$

which, for $Q=0$, becomes

$$V_{\alpha\beta}=(-)^{\beta-1/2}(2/5)^{1/2}\left(\frac{p_0+m}{2m}\right)^{1/2}g_5\frac{p^3}{p_0+m}d_{\alpha,\beta}{}^{5/2}(\theta)\,. \tag{26}$$

It follows that

$$\Gamma_{5/2}=\frac{2}{15}\frac{p^7}{M(p_0+m)}\frac{g_5{}^2}{4\pi}; \tag{27}$$

so, for $\Gamma_{5/2}=80$ MeV, $g_5{}^2/4\pi=0.0333\mu^{-4}$.

For $N_R=\frac{3}{2}^+$ the helicity amplitudes for the diagram are given by Eqs. (2), (20), and (23):

$$\langle\alpha,\lambda|M_{31}|\beta\rangle=(-)^{\lambda+\alpha-\beta}\frac{4\pi}{3}fg_3\left(\frac{p_0+m}{2m}\right)^{1/2}p^3\int_{-1}^{1}\frac{d\cos\theta}{t-\mu^2}d_{\alpha-\lambda,\beta}{}^J(\theta)d_{-\alpha,-\beta}{}^{3/2}(\theta)d_{\lambda,0}{}^2(\theta)\,. \tag{28}$$

We make use of

$$t-\mu^2=2pQ(\cos\theta-x)\,, \tag{29}$$

where

$$x=(2p_0Q_0+\mu^2-M^2-m^2)/2pQ\,.$$

Formula (28) then is easy to evaluate; since we are at $w=w_3(Q=0)$, only $J\otimes\frac{3}{2}\otimes 2=0$ contributes.[8] (In fact this relates directly to our assumption of an $L=0$ N_Rf state.) The result is

$$\langle\alpha,\lambda|M_{31}|\beta\rangle=-(-)^{\lambda+\alpha-\beta}\frac{8\pi}{3}fg_3\left(\frac{p_0+m}{2m}\right)^{1/2}p^3(2Mp_0+\mu^2-M^2-m^2)^{-1}(J,\alpha-\lambda,\tfrac{3}{2},-\alpha|J,\tfrac{3}{2},2,-\lambda)$$
$$\times(J,\beta,\tfrac{3}{2},-\beta|J,\tfrac{3}{2},2,0)(2,\lambda,2,-\lambda|2,2,0,0)(2,0,2,0|2,2,0,0)\,. \tag{30}$$

According to Table II there are 10 J^+ amplitudes; these are

$$M_{31}{}^\eta=-(-)^{\alpha-1/2}\frac{16\pi}{15}fg_3\left(\frac{p_0+m}{2m}\right)^{1/2}p^3(2Mp_0+\mu^2-M^2-m^2)^{-1}$$
$$\times(J,\alpha-\lambda,\tfrac{3}{2},-\alpha|J,\tfrac{3}{2},2,-\lambda)(J,\tfrac{1}{2},\tfrac{3}{2},-\tfrac{1}{2}|J,\tfrac{3}{2},2,0)\,, \tag{31}$$

where η depends on α, λ as shown in the table. From Eqs. (5) and (16), we obtain

$$d_\eta=(-)^{\alpha-1/2}(16\pi/15)fg_3p^3(w_3-w_1)(2Mp_0+\mu^2-M^2-m^2)^{-1}((p_0+m)/p)^l$$
$$\times(J,\alpha-\lambda,\tfrac{3}{2},-\alpha|J,\tfrac{3}{2},2,-\lambda)(J,\tfrac{1}{2},\tfrac{3}{2},-\tfrac{1}{2}|J,\tfrac{3}{2},2,0)\,, \tag{32}$$

[8] A. R. Edmonds, *Angular Momentum in Quantum Mechanics* (Princeton University Press, Princeton, New Jersey, 1960).

where l is given in Table III. It is worth noting that the η dependence of $d_\eta{}^2$ is contained entirely in the first Clebsch-Gordan coefficient and, moreover, that

$$\sum_\eta (J, \alpha-\lambda, \tfrac{3}{2}, -\alpha | J, \tfrac{3}{2}, 2, -\lambda)^2 = \tfrac{5}{2}. \tag{33}$$

For $N_R=\frac{5}{2}^+$ the analog of Eq. (28) is

$$\langle \alpha,\lambda | M_{31} | \beta \rangle = (-)^{\lambda+\alpha-1/2} \frac{4\pi}{\sqrt{15}} f g_5 \left(\frac{p_0+m}{2m}\right)^{1/2} \frac{p^5}{p_0+m} \int_{-1}^{1} \frac{d\cos\theta}{t-\mu^2} d_{\alpha-\lambda,\beta}{}^J(\theta) d_{-\alpha,-\beta}{}^{5/2}(\theta) d_{\lambda,0}{}^2(\theta) \tag{34}$$

and, by the same manipulations, we get, for the 15 coefficients

$$d_\eta = (-)^{\alpha-1/2} \frac{16\pi}{5\sqrt{15}} f g_5 \frac{p^5}{p_0+m} (w_3-w_1)(2Mp_0+\mu^2-M^2-m^2)^{-1} \left(\frac{p_0+m}{p}\right)^l$$
$$\times (J, \alpha-\lambda, \tfrac{5}{2}, -\alpha | J, \tfrac{5}{2}, 2, -\lambda)(J, \tfrac{1}{2}, \tfrac{5}{2}, -\tfrac{1}{2} | J, \tfrac{5}{2}, 2, 0). \tag{35}$$

We can now indicate why the recurrence states are the most attractive ones. Given $L=0$, the recurrences correspond to the largest J; this in turn calls for the largest l, although occasionally (e.g., with $N_R=\frac{3}{2}^+$) the next largest J may have the same l. Where l is largest the factor $[(p_0+m)/p]^l$ is dominant. In the case of a competing J having the same l, the second Clebsch-Gordan coefficient in (32) and (35) always favors the recurrence state. These remarks are not restricted to the two resonances we are treating here, but hold quite generally.

C. Results

We now look for a resonance between w_1 and w_3; accordingly, we compute $\mathrm{Re}\mathfrak{D}_0(w)$ and look for an energy $w=w^*$ such that (15) holds. The results for $J=\frac{7}{2}^+$ $(T=\frac{3}{2})$ and $J=\frac{9}{2}^+$ $(T=\frac{1}{2})$ are shown in Figs. 4 and 5, respectively. According to the model described in this section (the one conjectured to apply in extension of the model of Ref. 3), we find that the resonances occur at $w_{7/2}{}^*=11.8\,\mu$ (1650 MeV) and at $w_{9/2}{}^*=9.6\,\mu$ (1340 MeV). It is clear that the conjectured mechanism is sufficiently attractive (evidently, too much so). The positioning of the resonances leaves something to be desired; especially unpleasant is the occurrence of the $\frac{9}{2}^+$ below the $\frac{7}{2}^+$. Even if we use $\Gamma_{5/2}=42$ MeV (the result of Ref. 3) we can only increase the mass of the $\frac{9}{2}^+$ by 100 MeV.

The widths of the resonances may be computed from $\mathrm{Im}\mathfrak{D}_0$ and $(d/dw)(\mathrm{Re}\mathfrak{D}_0)$. For $\frac{7}{2}^+$ we find $\Gamma_{7/2}=26.5$ MeV; this differs by only a factor of 2 from the observed partial width for $N\pi$ decay.[1] We cannot expect our calculation to yield a result comparable with the observed total width since many inelastic channels that are open and important have been neglected in the model. In fact the very large inelasticity of both $\frac{7}{2}^+$ and $\frac{9}{2}^+$ resonances will be exploited as motivation for a different approach in the next section. The computed width of the $\frac{9}{2}$ resonance is unreasonably small; h-wave phase space and the very low resonance energy account for this.

III. THE COUPLED $N_R\pi$, N_Rf PROBLEM

The force pictured in Fig. 1 perhaps does not represent the extension of the model of Ref. 3 which is most relevant, although it is the most natural if we wish to compare our results with the resonances as observed in $N\pi$ scattering. For both the $\frac{7}{2}^+$ (1920 MeV) and the $\frac{9}{2}^+$?(2190 MeV) the elastic decay fractions are small, in the neighborhood of 30%,[1] indicating that the resonant $N\pi$ phase passes through 0 rather than $\frac{1}{2}\pi$.[9] Thus we might

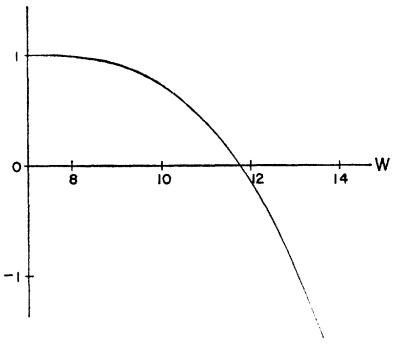

FIG. 4. $\mathrm{Re}\mathfrak{D}_0$ versus w for $\frac{7}{2}^+(T=\frac{3}{2})$.

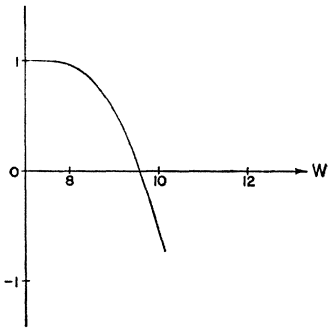

FIG. 5. $\mathrm{Re}\mathfrak{D}_0$ versus w for $\frac{9}{2}^+(T=\frac{1}{2})$.

[9] A thorough discussion of this effect may be found in, e.g., M. B. Watson, M. Ferro-Luzzi, and R. D. Tripp, Phys. Rev. 131, 2248 (1963).

assume, from this apparently weak coupling to the $N\pi$ channel, that the resonances are more appropriately to be sought in another channel.[10] We shall adopt the point of view in this section that this other channel is $N_R\pi$. Accordingly we assume the force of Fig. 2 to be the relevant extension of the model employed for the first nucleon recurrence.[3]

To pursue these observations we now look for the occurrence of a resonant state in $N_R\pi$ "elastic" scattering. We ignore channel 1 and add channel 2, the $N_R\pi$ channel. The $\mathfrak{F}$ matrix becomes

$$\mathfrak{F}=\begin{pmatrix} F_{22}{}^{sr} & F_{23}{}^{s\xi} \\ F_{32}{}^{\eta r} & F_{33}{}^{\eta\xi} \end{pmatrix} \tag{36}$$

in which, e.g.,

$$F_{32}{}^{\eta r}=\left(\frac{2M}{P_0+M}\right)^{1/2}\left(\frac{2M}{Q_0+M}\right)^{1/2}\left(\frac{P_0+M}{P}\right)^{l}M_{32}{}^{\eta r}, \tag{37}$$

where P_0 and P denote the N_R energy and momentum in the $N_R\pi$ state. The indices r and s run through the $\frac{1}{2}(2j+1)$ values needed to label all the amplitudes in conjunction with the $\frac{5}{2}(2j+1)$ integers η and ξ. The identification of these indices with the combinations of helicity amplitudes is still given by Table II if we replace the initial helicity state $|\frac{1}{2}\rangle$ by the set of $\frac{1}{2}(2j+1)$ states $|j\rangle$, $|j-1\rangle,\cdots,|\frac{1}{2}\rangle$.

The nonzero forces of the model are assumed to be

$$\begin{aligned} \mathrm{disc}_L F_{32}{}^{\eta r}&=2\pi i c_\eta b_r \delta(w-w_2), \\ \mathrm{disc}_L F_{23}{}^{s\xi}&=2\pi i b_s c_\xi \delta(w-w_2); \end{aligned} \tag{38}$$

we shall demonstrate the validity of factoring the coefficients later. The determinant of the $\mathfrak{D}$ matrix in this case is

$$\mathfrak{D}_0=1-b^2c^2(w-w_2)^2S_2(w)T_2(w), \tag{39}$$

where

$$\begin{aligned} b^2&=\sum_r b_r{}^2, \\ c^2&=\sum_\eta c_\eta{}^2, \end{aligned} \tag{40}$$

and where

$$\begin{aligned} S_2(w)&=\int_{M+\mu}^{\infty}\frac{dx}{(x-w)}\frac{\rho_2(x)}{(x-w_2)^2} \\ \text{and}\qquad T_2(w)&=\int_{M+\Delta}^{\infty}\frac{dx}{(x-w)}\frac{\rho_3(x)}{(x-w_2)^2}. \end{aligned} \tag{41}$$

In S_2 we use

$$\rho_2=\frac{2}{(4\pi)^3}\frac{P^{2l+1}}{w(P_0+M)^{2l-1}}, \tag{42}$$

and we take $l=3$ for both $J=\frac{7}{2}$ and $\frac{9}{2}$.

Once again the parameters of the model are determinable in terms of coupling constants; this time we compute the projections of the diagram of Fig. 2. Here the dominant singularity occurs at $w=M+\mu$, where P vanishes; so we choose $w_2=M+\mu$. We determine the factor b^2c^2 at $w=w_3$ from

$$c_\eta b_r=(w_2-w_3)[F_{32}{}^{\eta r}(w_3)]_{\text{diagram}}. \tag{43}$$

For the $N_{3/2}{}^*N_{3/2}{}^*\pi$ vertex we use

$$V_{\alpha\beta}=g_{33}\bar{\psi}^\alpha{}_\mu(Q)\gamma_5\psi^\beta{}_\mu(P); \tag{44}$$

in so doing, we are neglecting the f-wave coupling (presumably small due to the centrifugal-barrier effect). For $Q=0$ this leads to

$$\begin{aligned} V_{\alpha\beta}=(-)^{\beta+1/2}\epsilon_\beta g_{33}&[(P_0+M)/2M]^{1/2} \\ &\times[P/(P_0+M)]d_{\alpha,\beta}{}^{3/2}(\theta), \end{aligned} \tag{45}$$

where

$$\begin{aligned} \epsilon_{\pm 3/2}&=1, \\ \epsilon_{\pm 1/2}&=\tfrac{1}{3}(1-2P_0/M). \end{aligned} \tag{46}$$

The helicity amplitudes at $w=w_3$ are

$$\begin{aligned} \langle\alpha,\lambda|M_{32}|\beta\rangle=&-(-)^{\alpha+1/2}\tfrac{4}{5}\pi(\tfrac{2}{3})^{1/2}fg_{33} \\ &\times\left(\frac{P_0+M}{2M}\right)^{1/2}\epsilon_\beta\frac{P^3}{P_0+M}(2MP_0+\mu^2-2M^2)^{-1} \\ &\times(J,\alpha-\lambda,\tfrac{3}{2},-\alpha|J,\tfrac{3}{2},2,-\lambda) \\ &\times(J,\beta,\tfrac{3}{2},-\beta|J,\tfrac{3}{2},2,0). \end{aligned} \tag{47}$$

Then, for $r=\frac{3}{2},\frac{1}{2}$ and for $\eta=1$ to 10, the calculation of the J^+ amplitudes and the application of Eq. (43) yields the coefficients

$$\begin{aligned} c_\eta=(-)^{\alpha+1/2}&\frac{8\pi}{5}(\tfrac{2}{3})^{1/2}fg_{33}\frac{P^3}{P_0+M} \\ &\times(w_3-w_2)(2MP_0+\mu^2-2M^2)^{-1}\left(\frac{P_0+M}{P}\right)^{l} \\ &\times(J,\alpha-\lambda,\tfrac{3}{2},-\alpha|J,\tfrac{3}{2},2,-\lambda) \end{aligned} \tag{48}$$

and

$$b_r=\epsilon_r(J,r,\tfrac{3}{2},-r|J,\tfrac{3}{2},2,0). \tag{49}$$

The factorization assumed in (38) is evidently valid by inspection of Eq. (47); this circumstance holds equally well for $N_R=\frac{5}{2}^+$.

For the $N_{5/2}{}^*N_{5/2}{}^*\pi$ vertex we neglect f-wave and h-wave couplings and write

$$V_{\alpha\beta}=g_{55}\bar{\psi}^\alpha{}_{\mu\nu}(Q)\gamma_5\psi^\beta{}_{\mu\nu}(P). \tag{50}$$

For $Q=0$, this becomes

$$\begin{aligned} V_{\alpha\beta}=(-)^{\beta-1/2}\tau_\beta g_{55}&[(P_0+M)/2M]^{1/2} \\ &\times[P/(P_0+M)]d_{\alpha,\beta}{}^{5/2}(\theta), \end{aligned} \tag{51}$$

where

$$\begin{aligned} \tau_{\pm 5/2}&=1, \\ \tau_{\pm 3/2}&=\tfrac{1}{5}(1-4P_0/M), \\ \tau_{\pm 1/2}&=\tfrac{1}{5}(1-2P_0/M+2P_0{}^2/M^2). \end{aligned} \tag{52}$$

[10] We are grateful to R. H. Capps for suggesting this notion.

The helicity amplitudes at $w=w_3$ are

$$\langle\alpha,\lambda|M_{32}|\beta\rangle=-(-)^{\alpha-1/2}\tfrac{4}{5}\pi(\tfrac{2}{3})^{1/2}fg_{55}$$
$$\times\left(\frac{P_0+M}{2M}\right)^{1/2}\tau_\beta\frac{P^3}{P_0+M}(2MP_0+\mu^2-2M^2)^{-1}$$
$$\times(J,\alpha-\lambda,\tfrac{5}{2},-\alpha|J,\tfrac{5}{2},2,-\lambda)$$
$$\times(J,\beta,\tfrac{5}{2},-\beta|J,\tfrac{5}{2},2,0). \quad (53)$$

Thus, for the case $N_R=\frac{5}{2}^+$,

$$c_\eta=(-)^{\alpha-1/2}\frac{8\pi}{5}(\tfrac{2}{3})^{1/2}fg_{55}\frac{P^3}{P_0+M}$$
$$\times(w_3-w_2)(2MP_0+\mu^2-2M^2)^{-1}((P_0+M)/P)^l$$
$$\times(J,\alpha-\lambda,\tfrac{5}{2},-\alpha|J,\tfrac{5}{2},2,-\lambda) \quad (54)$$

and

$$b_r=\tau_r(J,r,\tfrac{5}{2},-r|J,\tfrac{5}{2},2,0), \quad (55)$$

in which

$$r=\tfrac{5}{2},\tfrac{3}{2},\tfrac{1}{2} \quad \text{and} \quad \eta=1 \text{ to } 15.$$

The coupling constants g_{33} and g_{55} are not experimentally determined; we shall let them be variable parameters for the time being and determine $g_{33}^2/4\pi$ and $g_{55}^2/4\pi$ as functions of the resonance positions. To this end we define the quantity G^2 from Eq. (39) by writing

$$\mathrm{Re}\mathfrak{D}_0=1-g^2G^2/4\pi, \quad (56)$$

where $g=g_{33}$ for $J=\frac{7}{2}$ and $g=g_{55}$ for $J=\frac{9}{2}$. At resonance we then have

$$g^2/4\pi=[G^2(w^*)]^{-1}. \quad (57)$$

The right-hand side of Eq. (57) is plotted in Fig. 6 for $\frac{7}{2}^+$ and in Fig. 7 for $\frac{9}{2}^+$. For $w_{7/2}{}^*=13.7\,\mu$ (1920 MeV) and $w_{9/2}{}^*=15.6\,\mu$ (2190 MeV) we obtain

$$g_{33}^2/4\pi=36.7$$

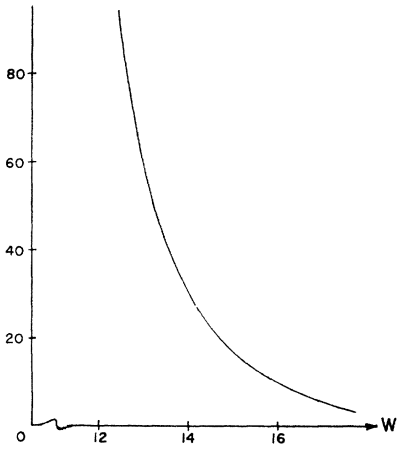

FIG. 6. 33 coupling constant as a function of resonance energy.

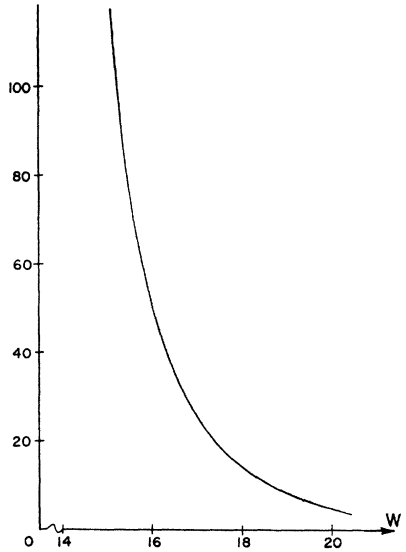

FIG. 7. 55 coupling constant as a function of resonance energy.

and

$$g_{55}^2/4\pi=69. \quad (58)$$

If we allow a tolerance of about 0.5 μ in the ability of our model to give resonance energies we can see from the figures that we have sufficient sensitivity of the results to give a range of 26 to 51 for the 33 coupling and of 48 to 116 for the 55 coupling.

Something can be said about what to expect for the 33 coupling if we invoke a form of $SU(6)$ symmetry. The couplings g and g_{33} (and g_3 as well) are related since the N and $N_{3/2}{}^*$ are both supposed to belong to the 56-dimensional $SU(6)$ multiplet.[11] We shall refer to the results of Capps[12] who has adopted a static model for the meson-baryon vertices. The "decay" vertex for $N^*\to N^*\pi$ may be written

$$V_{N^*,N^*\pi}=\langle 56,10|B_{10}P_8,10\rangle\langle B_{10}P_8,10|N^*\pi\rangle V_{56}$$
$$=(\tfrac{1}{6}\sqrt{10})V_{56}; \quad (59)$$

and for $N\to N\pi$

$$V_{N,N\pi}=[\langle 56,8|B_8P_8,8_a\rangle\langle B_8P_8,8_a|N\pi\rangle$$
$$+\langle 56,8|B_8P_8,8_s\rangle\langle B_8P_8,8_s|N\pi\rangle]V_{56}$$
$$=(\tfrac{1}{6}\sqrt{10})V_{56}. \quad (60)$$

In these expressions the first factors are the Clebsch-Gordan coefficients in Capps' wave functions, the second factors are the appropriate isoscalar coefficients,[13] and the last factor V_{56} denotes the reduced matrix element. Thus for degenerate masses the ratio of the "decay" probabilities is 1. On the other hand, if we compute this ratio from (45) and from its analog for $N\to N\pi$ in the

[11] F. Gürsey, A. Pais, and L. A. Radicati, Phys. Rev. Letters **13**, 299 (1964); B. Sakita, Phys. Rev. **136**, B1756 (1964).

[12] R. H. Capps, Phys. Rev. Letters **14**, 31 (1965). See also J. G. Belinfante and R. E. Cutkosky, *ibid.* **14**, 33 (1965).

[13] J. J. de Swart, Rev. Mod. Phys. **35**, 916 (1963).

static limit, we get $(5/9)g_{33}^2/g^2$, and, hence we conclude that

$$g_{33}^2/4\pi=(9/5)g^2/4\pi. \quad (61)$$

Numerically, then, we have $g_{33}^2/4\pi=27$ and, from this, the model gives a $\frac{7}{2}$ resonance at $w_{7/2}^*=14.2\,\mu$ (1988 MeV), in rather good agreement with experiment. Unfortunately no such symmetry argument is at our disposal for the 55 coupling.

IV. CONCLUSIONS

There is at least one sense in which we can say we have a recurrence mechanism. We are dealing with a model which is, by definition, attractive in every state. We have shown that the attraction is maximal in the recurrence state. Our original conjecture[3] that the force of Fig. 1 provides the mechanism is therefore qualitatively successful. Our $\frac{7}{2}^+$ resonance however is two pion masses off the mark.

The comparatively weak observed coupling to the $N\pi$ system of both the 1920- and 2190-MeV resonances suggests that we should formulate our model from the point of view of looking for resonant states in another channel. Accordingly we couple $N_R\pi$ and N_Rf states, and indeed we obtain vastly improved results.

The model, in both its original and its improved form, fails to touch upon the important question of calculating the elasticity of the resonances. To study this entails including open inelastic channels with couplings such that the elastic phase can be driven through 0, in agreement with the observed small elasticity.[9] The formulation of a three-channel model with special application to this problem is treated in a subsequent paper.

Our models are based on the role of the f meson in specially chosen inelastic states. The mechanism is altogether different from other explanations in the literature for the pattern of quantum numbers of the observed excited nucleonic states. Carruthers,[14] and Donnachie and Hamilton[15] have analyzed many exchange forces and conclude that the signs and sizes of these imply attraction in all the right states. Carruthers in particular shows how the reciprocal bootstrap of Chew[16] has a natural extension to the recurrence states among the higher resonances. His forces have not yet been implemented by a unitary calculation to ascertain the positions of the resonances. Freedman[17] has given a dynamical model for the nucleon trajectory which incorporates inelastic effects. His choice of inelastic states differs from ours and the calculation invokes only elastic unitarity.

ACKNOWLEDGMENTS

The authors are grateful to C. H. Albright and R. H. Capps for informative conversations contributing to this research.

[14] P. Carruthers, Phys. Rev. Letters **10**, 538 (1963); **10** 540 (1963); Phys. Rev. **133**, B497 (1964).
[15] A. Donnachie and J. Hamilton, Ann. Phys. (N.Y.) **31**, 410 (1965).
[16] G. F. Chew, Phys. Rev. Letters **9**, 233 (1962).
[17] D. Z. Freedman, Phys. Rev. **134**, B652 (1964).